

GA-A22864

**THE ROLE OF NEUTRALS IN THE H-L BACK  
TRANSITION OF HIGH DENSITY SINGLE-NULL AND  
DOUBLE-NULL GAS-FUELED DISCHARGES IN DIII-D**

by

**T.W. PETRIE, R. MAINGI, G.D. PORTER, S.L. ALLEN, M.E.  
FENSTERMACHER, R.J. GROEBNER, D.N. HILL, A.W. LEONARD,  
C.J. LASNIER, M.A. MAHDAVI, R.A. MOYER, M.E. RENSINK,  
D.M. THOMAS, W.P. WEST, and the DIII-D TEAM**

**AUGUST 1998**

## DISCLAIMER

This report was prepared as an account of work sponsored by an agency of the United States Government. Neither the United States Government nor any agency thereof, nor any of their employees, makes any warranty, express or implied, or assumes any legal liability or responsibility for the accuracy, completeness, or usefulness of any information, apparatus, product, or process disclosed, or represents that its use would not infringe privately owned rights. Reference herein to any specific commercial product, process, or service by trade name, trademark, manufacturer, or otherwise, does not necessarily constitute or imply its endorsement, recommendation, or favoring by the United States Government or any agency thereof. The views and opinions of authors expressed herein do not necessarily state or reflect those of the United States Government or any agency thereof.

# THE ROLE OF NEUTRALS IN THE H-L BACK TRANSITION OF HIGH DENSITY SINGLE-NULL AND DOUBLE-NULL GAS-FUELED DISCHARGES IN DIII-D

by

T.W. PETRIE, R. MAINGI,<sup>†</sup> G.D. PORTER,<sup>‡</sup> S.L. ALLEN,<sup>‡</sup>  
M.E. FENSTERMACHER,<sup>‡</sup> R.J. GROEBNER, D.N. HILL,<sup>‡</sup> A.W. LEONARD,  
C.J. LASNIER,<sup>‡</sup> M.A. MAHDAVI, R.A. MOYER,<sup>◇</sup> M.E. RENSINK,<sup>‡</sup>  
D.M. THOMAS, W.P. WEST, and the DIII-D TEAM

This is a preprint of a paper to be presented at the 13th International Conference on Plasma Surface Interactions on Controlled Fusion Devices, May 18–23, 1998, San Diego, California and to be published in *Journal of Nuclear Materials*.

<sup>†</sup>Oak Ridge National Laboratory

<sup>‡</sup>Lawrence Livermore National Laboratory

<sup>◇</sup>University of California, San Diego

Work supported by  
the U.S. Department of Energy  
under Contracts DE-AC03-89ER51114, DE-AC05-96-OR22464,  
W-7405-ENG-48, and Grant DE-FG03-95ER54294

GA PROJECT 3466  
AUGUST 1998

**ABSTRACT**

The role of neutrals in triggering the H–L back transition in high density ELMing H–mode plasmas is explored in double-null (DN) and single-null (SN) divertors. We propose that the neutral particle buildup below the X–point may play an important role in triggering the H–L transition at high density. Neutral pressure in the private flux region is, in fact, significant near the H–L backtransition (10–40 mTorr, except at very low input power). High density formation inside the separatrix near the X–point may also be a factor in triggering the H–L backtransition. We have observed that the ELMing H–mode density limit in SN divertors normally occurred at or near the H–L back transition, where  $\bar{n}_{e,HL} \propto P_{in}^{0.1}/B_t^{0.5}$ , for  $I_p=1$  MA,  $B_t=1.1\text{--}2.1$  T,  $q_{95}=3\text{--}6$ ,  $P_{in}=3\text{--}12$  MW. The radiated power coming from inside the separatrix at the H–L transition did not appear sufficient by itself to produce this back transition, since it is only  $\sim 15\text{--}30\%$  of  $P_{in}$ .

Poloidally-localized neutrals may explain two important differences in SN and double-null (DN) plasmas near their respective H–L backtransitions. First, electron pressure along the separatrix between the X–point and the outboard strike point decreased only modestly for DN divertors, even at densities comparable to the Greenwald density limit  $\bar{n}_{e,G}$ , in contrast to SN plasmas. Second, no divertor (or core) MARFEs were detected in the DNs as  $\bar{n}_e$  approaches  $\bar{n}_{e,G}$ , in contrast to SNs, where divertor MARFEs can form at  $\bar{n}_e/\bar{n}_{e,G}$  as low as  $\sim 0.6$ . High X–point DNs achieved density limits well above those of comparably-prepared SNs, e.g.,  $\bar{n}_e/\bar{n}_{e,G} \approx 0.9\text{--}1.0$  for DNs versus  $0.75\text{--}0.80$  for SNs. These differences result from a lower neutral pressure in the private flux regions of DNs than in comparable SNs at the same  $\bar{n}_e$ , since neutrals impact both pressure balance and MARFEing behavior.

## 1. INTRODUCTION

The addition of cold deuterium gas into single-null (SN) ELMing H–mode diverted plasmas can trigger the formation of low-temperature ( $\sim 1\text{--}2$  eV), high density ( $\gtrsim 2 \times 10^{20}$  m<sup>-3</sup>), highly radiating region located between the X–point and the divertor floor [1–3]. Because the formation of this high density region has similarities with MARFE behavior [4], we refer to it as a “divertor MARFE” and the conditions under which it occurs as the “Partially Detached Divertor” (PDD) regime [3]. While some details may differ, other tokamaks, such as Alcator C-MOD [5], JET [6], and ASDEX-Upgrade [7] have reported similar observations. Continued gas puffing during SN PDD operation produces a transition back to the L–mode regime. This “back transition” is characterized by a cessation of ELMing activity and a drop in edge plasma density.

While much of tokamak research currently is focused on plasma behavior in SNs, future generation tokamaks may require double-null (DN) divertor configurations to achieve “high performance” characteristics [8], such as enhanced energy confinement and high plasma  $\beta$ . Some “high performance” scenarios, moreover, may necessitate DN operation at densities where PDD conditions could exist, at least based on SN extrapolations. For this reason, the question of whether high density behavior in SNs can be used to predict high density behavior in DNs needs to be addressed. In this paper we examine this issue, particularly the role that the poloidal distribution of the neutral particles might play. After describing our basic experimental setup in Section 2, we detail the important characteristics of high density PDD SNs in Section 3 and contrast these with high density DNs in Section 4. In Section 5, we discuss our results.

## 2. EXPERIMENTAL SETUP

The SN and balanced DN plasma configurations discussed in this paper are shown in Fig. 1(a,b). Both are representative of low triangularity ( $\delta_T \approx 0.4$ ) discharges with moderate separation of the X-point from the divertor tiles ( $h_{X\text{-point}} \approx 0.12$  m). By “balanced” we mean that the radial separation of the separatrices for the upper and lower divertor as projected back and measured at the outer midplane is  $\leq 0.1$  cm. We focus on low triangularity configurations in both SN and DN for two main reasons. First, low triangularity SNs and DNs give the most favorable diagnostic coverage of the (lower) divertor plasma, especially with respect to measuring electron density and temperature (e.g., with the divertor Thomson scattering and Langmuir probe systems). Although no similar diagnostic capability exists in the upper divertor at present, an “upper divertor” density and temperature can be “measured,” in a manner of speaking, with the lower divertor diagnostics by reversing the toroidal field (and, hence, the grad-B drift direction). The second reason to focus on the low- $\delta_T$  DN mode is that it allows comparisons with a large database of low triangularity SN divertor plasmas.

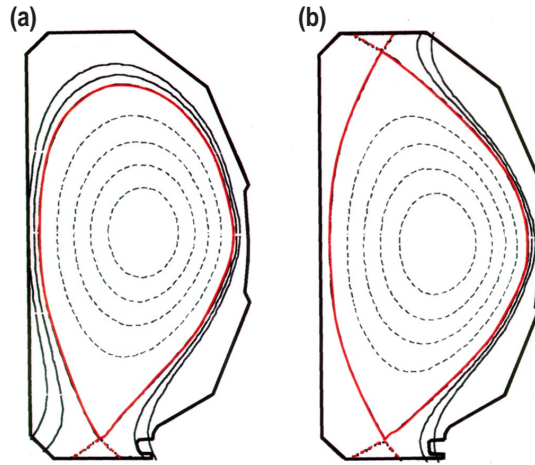


Fig. 1. (a) Representative single-null and (b) double-null configurations considered in this study are shown.

### 3. H–L TRANSITION IN SINGLE-NULLED DIVERTORS

Figure 2 describes the evolution of an ELMing single-null H–mode plasma during cold deuterium ( $D_2$ ) gas injection. The PDD was initiated at  $t=2.73$  s and the H–L backtransition occurred at  $t=3.32$  s. The latter is evidenced by a cessation of ELMing recycling activity [ $(D_{\alpha,div})$  in Fig. 2(b)] and a drop in the “edge” (pedestal) density [ $n_{e,ped}$  in Fig. 2(c)]. The PDD operating “window” (i.e., between the initiation of the PDD and the H–L back transition) for the line-averaged electron density [ $\bar{n}_e$  in Fig. 2(c)] was in the range  $\bar{n}_e/n_{e,G} = 0.82$  to  $0.98$ , where  $n_{e,G}$  ( $=I_p/\pi a^2$ ) is the Greenwald density limit [9]; typically, the width of this operating window for DIII–D plasmas is  $0.1$ – $0.2$  in units of  $\bar{n}_e/n_{e,G}$ . The density profile was flat to modestly peaked during most of the PDD mode, since the electron density measurement deep in the core plasma ( $n_{e,core}$ ) tracks  $\bar{n}_e$  and  $n_{e,ped}$  [Fig. 2(c)]. The  $n_e$ -profile became more peaked near the H–L limit, however, when  $n_{e,core}$  increased as  $n_{e,ped}$  decreased. Energy confinement shortly before the H–L transition was roughly  $40\%$ – $50\%$  lower than during pre-puff times [Fig. 2(d)]; typically,  $\tau_E/\tau_{E89-L} \approx 1.1$ – $1.3$  immediately preceding the H–L transition as defined above, where  $\tau_{E89-L}$  is the ITER89-L energy confinement [10].

For SN plasmas with lower safety factor values (e.g.,  $q_{95} \leq 4.5$ , as in this example), the back transition is preceded by the formation of a high density, low temperature region *inside* the separatrix near the X–point (“core MARFE”). This is indicated by the increase in electron density ( $n_{e,X-point} > 2 \times 10^{20} \text{ m}^{-3}$ ) and a drop in electron temperature ( $T_{e,X-point} < 5 \text{ eV}$ ) *inside* the separatrix (core plasma) near the X–point [i.e.,  $t \approx 3.15$  s in Fig. 2(e,f)]. During the H–mode phases, the core MARFEs do not penetrate more than  $5$  cm above the X–point; this represents  $< 1$  cm from the plasma edge when traced along a field line back to the midplane. The appearance of the core MARFE is coincident with a decrease in both  $n_{e,ped}$  and  $\tau_E/\tau_{E89-L}$ .

While total radiated power ( $P_{rad}$ ) near the H–L density limit  $\sim 80\%$  of the neutral beam power [ $P_{inj}$  in Fig. 2(g)], bolometric inversions indicate that most of this radiation occurs *outside* the separatrix. The radiated power from inside the separatrix (i.e., the “core” radiated power) is  $\approx 15\%$  of the input power for this shot; in general, the core radiated fraction is  $15\%$ – $30\%$  near the H–L density limit for SNs. Carbon was the principal impurity radiator. Typically, the carbon concentration in the core plasma is approximately  $1\%$  during the ELMing PDD.

Neutral pressure measured in the private flux region ( $P_N$ ) shortly before the H–L back transitions depends strongly on both input power and toroidal field (i.e.,  $\propto P_{input}^2/B_T^2$ ). For the DIII–D SNs, neutral pressure in the private flux region is typically in the tens of milli-torr range prior to the H–L transition. For example, for SNs with similar parameters to the DNs

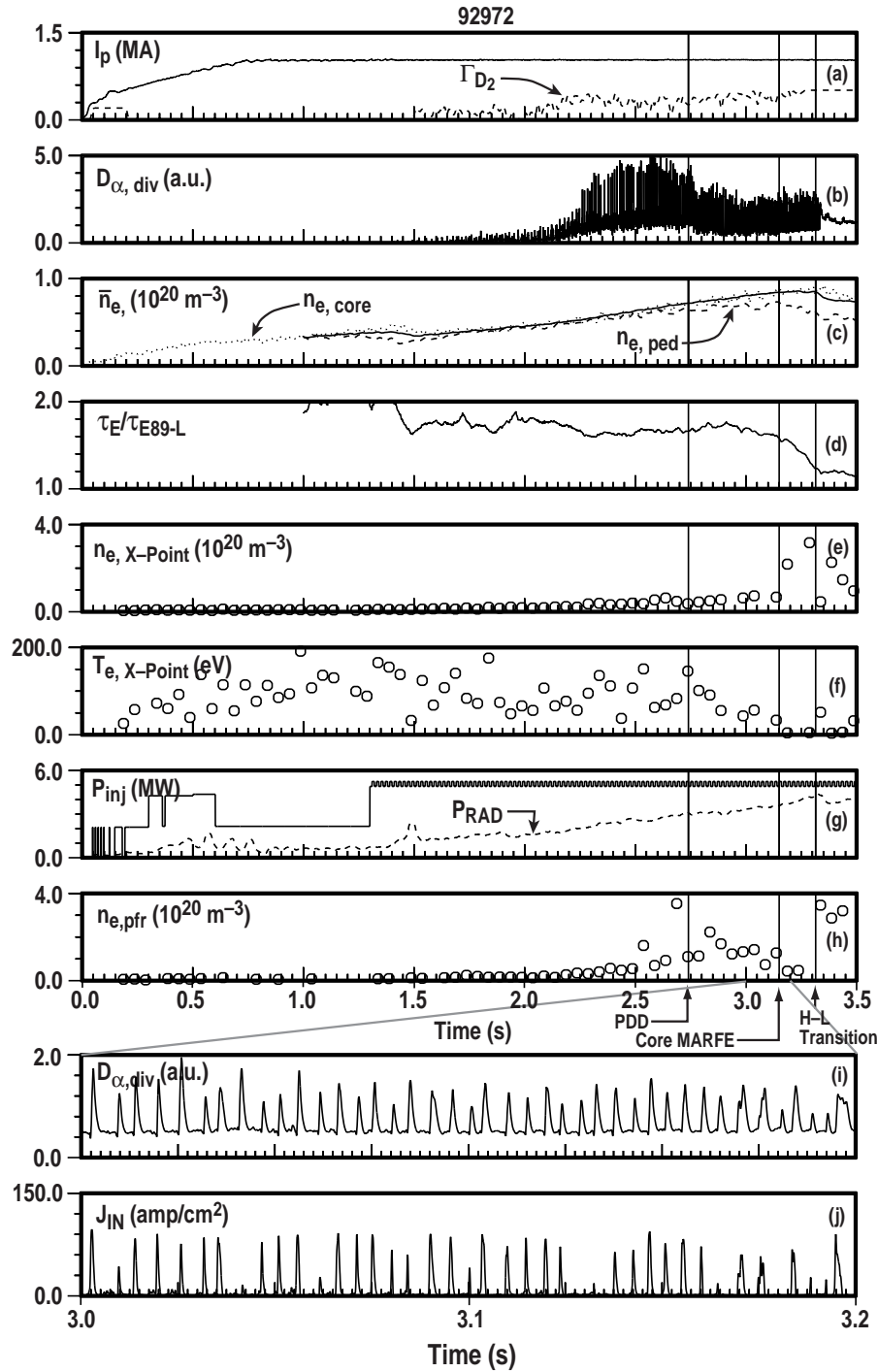


Fig. 2. Partially detached single-null divertor undergoes significant changes in both core and divertor behavior prior to the H-L transition:  $B_T = 2.1$  T,  $a = 0.61$  m,  $q_{95} = 3.2$ .  $D_{\alpha,div}$  indicates  $D_{\alpha}$  recycling activity in the divertor,  $\bar{n}_e$  is the line averaged density,  $n_{e,ped}$  is the pedestal density,  $n_{e,core}$  is electron density measured well inside the plasma core,  $n_{e,X-point}$  and  $T_{e,X-point}$  are electron density and temperature measured by Thomson scattering inside the core plasma near the separatrix,  $n_{e,pFR}$  is electron density measured by Thomson scattering in the private flux region half-way between X-point and the floor tiles under the X-point, and  $J_{in}$  is the saturation current under the inboard separatrix (Langmuir probes).

we consider next ( $P_{\text{input}} = 7$  MW,  $B_T = 2$  T, and  $I_p = 1.3$  MA),  $P_N$  prior to the H–L backtransition is  $\sim 40$  mTorr).

There was significant electron density in the private flux region; Fig. 2(h) shows  $n_{e,\text{pfr}} \approx 1\text{--}2 \times 10^{20} \text{ m}^{-3}$  during most of the PDD;  $n_{e,\text{pfr}}$  is measured half way between the X–point and the floor tiles directly under the X–point. During normal PDD operation the inboard divertor leg is totally detached *between* ELM pulses. During ELMs, however, the inboard leg in SNs re-attaches, as shown by the jump in the saturation current under the inboard leg [ $D_{\alpha,\text{div}}$  and  $J_{\text{in}}$  in Fig. 2(i,j)]. This transient re-attachment of the inboard leg may contribute to the buildup of high neutral density in the private flux region (PFR) by both supplying the recycling particles and then preventing their escape from the PFR.

## 4. SINGLE-NULL AND DOUBLE-NULL COMPARISONS

### 4.1. The H–L density limit for SN and DN divertors

Data obtained during recent experiments with SNs [11] indicate that the H–L density limit has a dependence on toroidal field [i.e.,  $\sim(B_t)^{-0.5}$ ] and only a weak dependence on input power [i.e.,  $\sim(P_{\text{input}})^\epsilon$ , where  $\epsilon \leq 0.1$ ]. This scaling is different than the Greenwald density limit for L–mode plasmas, as there is no toroidal field dependence in Greenwald scaling. After normalizing the H–L density limit to  $B_T$  and  $P_{\text{input}}$  and “windowing” on a common set of values for toroidal field, minor radius, and elongation, Fig. 3 shows that the H–L density limit in SNs (open circles) increases roughly linearly with  $I_p$ . The solid line is a linear best fit to the SN data. Also shown in Fig. 3 is a comparison of the H–L line-averaged density limits for SN- and DNs. The ensemble line-averaged density ( $\bar{n}_e$ ) for the DNs is  $\sim 15\%$  higher than for the SNs. This translates into a higher average Greenwald fraction (i.e.,  $\bar{n}_e/n_{eG}$ , where  $n_{eG}(10^{20} \text{ m}^{-3}) = I_p(\text{MA})/[\pi a(\text{m})]^2$ ) for the DNs (i.e.,  $\approx 0.9$ ) than for comparable SNs (i.e.,  $\lesssim 0.8$ ).

### 4.2. Global behavior of DNs at high density

Data from two high density, DN shots with opposite grad-B drift directions are plotted in Fig. 4. Both discharges were balanced during the times of interest. For later discussion of their divertor properties we have chosen a timeslice for each of these two shots at a common density value [i.e.,  $\bar{n}_e/n_{eG} \approx 0.95$ , as in Fig. 4(b)].

At this density,  $\tau_E/\tau_{E89}$  is  $\sim 1.6$  for both shots [Fig. 4(c)]. The rise in radiated power from the main plasma ( $P_{\text{rad,core}}$ ) largely accounts for this degradation in  $\tau_E$  during the gas puffing phase [Fig. 4(d)]. We observed higher radiated power in the divertor opposite the grad-B drift direction in the two timeslices selected. At these times the radiated power in the divertor/X–point region opposite the grad-B drift direction was  $\sim 10\%$ – $20\%$  higher than the power radiated in the opposite divertor [Fig. 4(e) and 4(f)]. Bolometric analysis has indicated that this divertor radiation was localized primarily along the outer leg of each divertor.

Neutral pressure in the private flux region ( $P_N$ ) is  $< 3$  mtorr for the high density times considered [Fig. 4(g)] and are at least an order of magnitude lower than comparable high density SN divertor discharges at a comparable  $\bar{n}_e$ . As with SN PDD discharges at high density, the *inboard* legs of the DN divertor at high density are virtually detached between ELMs, that is,

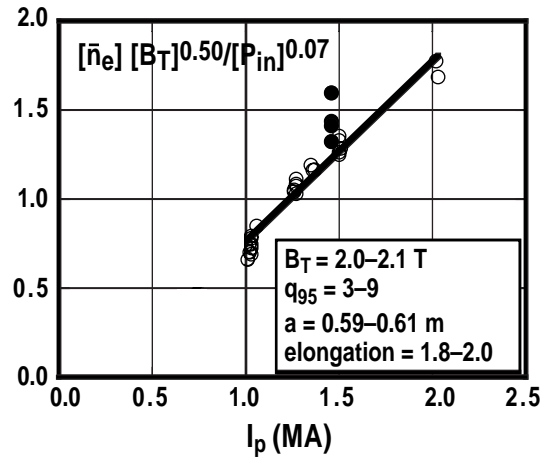


Fig. 3. The “normalized” H–L density limit is shown for single-null (open circles) and double-null (closed circles) as a function of plasma current. The line-averaged density ( $\bar{n}_e$ ) is in units of  $10^{20} \text{ m}^{-3}$ , the toroidal field ( $B_T$ ) is in Tesla, and the power input ( $P_{in}$ ) is in MW. The solid line is the linear best fit to the SN data.

particle and heat fluxes under the inboard separatrix strike point decreased. With gas injection, the saturation current under the inboard legs showed significantly reduced activity, and a measurably reduced effect from ELMs on particle flux [ $D_{\alpha,div}$  and  $J_{in}$  in Fig. 4(h,i)]. This latter effect is in contrast to what we have observed in SNs.

#### 4.3. Electron density and temperature in the divertor and at the X–point

It is instructive to take a closer look at the behavior of  $n_e$ ,  $T_e$ , electron pressure ( $P_e$ ) between the X–point and strike point along the outboard divertor separatrix for the  $\bar{n}_e/n_{eG} \approx 0.95$  cases above. There is no evidence of MARFE formation between the X–point and strike point [ $n_e$  in Fig. 5(a)];  $T_e$  along the separatrix was “cold” (i.e.,  $\approx 3\text{--}4 \text{ eV}$ ) only near the strike point [Fig. 5(b)]. That the electron temperature has cooled to  $< 5 \text{ eV}$  near the strike point, however, suggests that a divertor MARFE or “partial detachment” may be near. There was a modest reduction in the electron pressure ( $P_e$ ) along the separatrix between the X–point and the strike point [Fig. 5(c)];  $P_e$  between the X–point and the strike point for the DN prior to gas puffing is added for comparison (dashed line). For SNs during the PDD, the reduction in  $P_e$  during the PDD is typically higher (factor of  $\sim 6$ ) [12].

The lack of a core MARFE at high densities (even near the H–L back transition) suggests that electron temperatures near either X–point (inside the separatrix) should be significantly higher than what one has found in SNs during high density (PDD) operation. The lack of a core

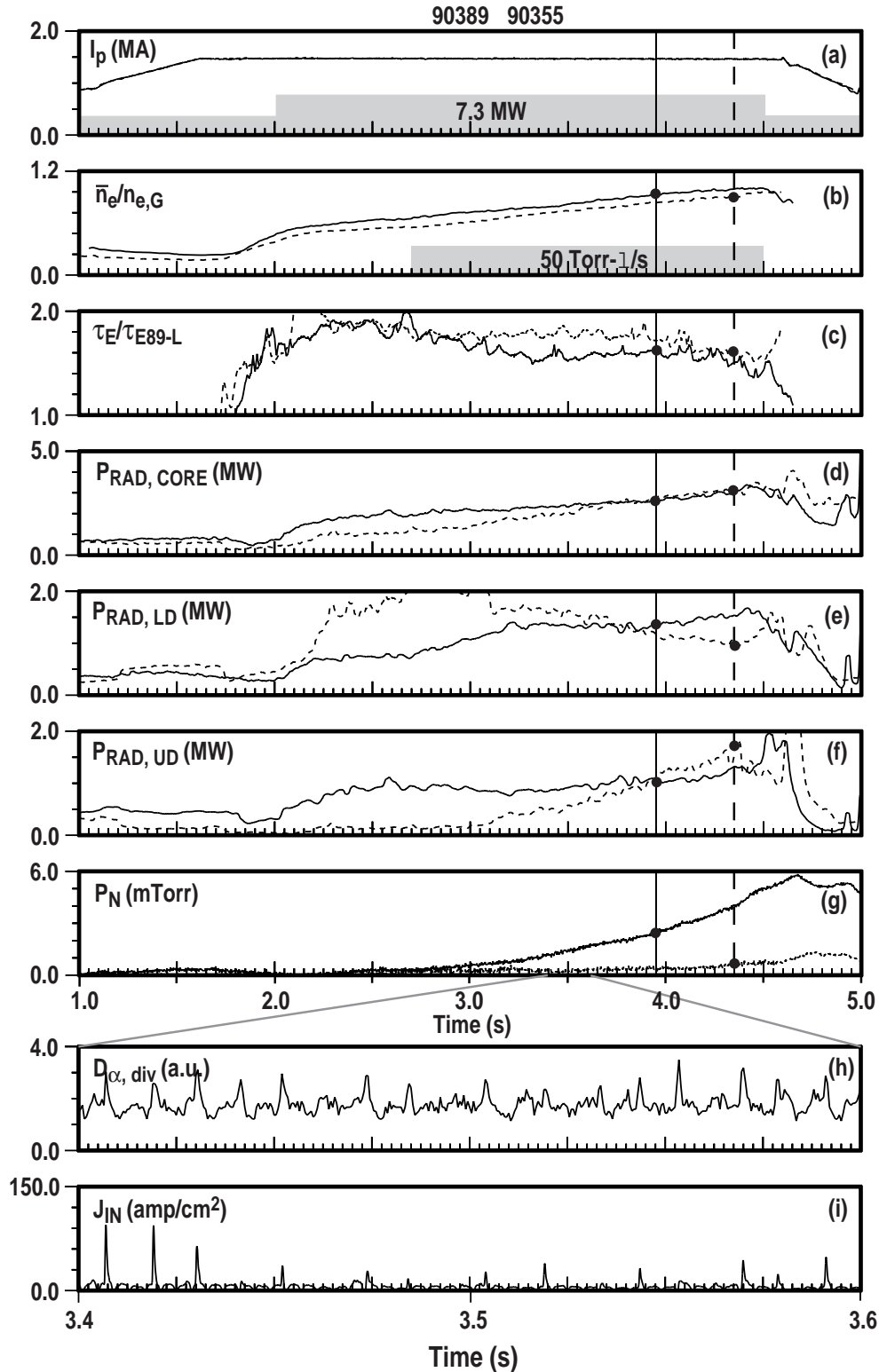


Fig. 4. Two high density ( $\bar{n}_e/n_{e,G} = 0.95$ ) double-null discharges with opposite  $\nabla B$ -drift directions shows some asymmetry in radiated power:  $\nabla B$ -drift toward the upper divertor (solid) and  $\nabla B$ -drift toward the lower divertor (dashed),  $B_T = 2.1$  T,  $a = 0.61$  m,  $q_{95} \sim 4.5$ .  $J_{in}$  is the saturation current near the inboard separatrix strike point from the shot with  $\nabla B$ -drift toward the upper divertor.

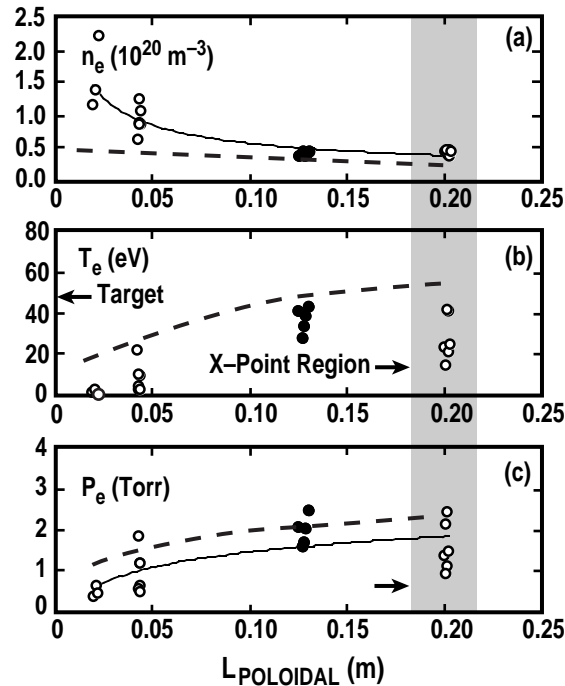


Fig. 5. A composite of the high density DN shots shown in Fig. 4 plots (a) electron density, (b) temperature, and (c) pressure versus poloidal length along the outboard separatrix between the X–point and strike point. The solid circles are data from the  $\nabla B$ -drift toward the lower divertor; the open circles are data from the  $\nabla B$ -drift toward the upper divertor. Data prior to gas puffing is represented by the dashed curves. PDD behavior is not observed.

MARFE is understandable from the measurement of  $T_e$ . For example, for the high density time slices in Fig. 4, the electron temperatures inside the separatrices at either of the X–points were still  $\geq 50$  eV, well above temperatures where one might expect X–point MARFEs to form [12]. No evidence of a reduction of electron pressure *inside* the separatrix near either X–point during gas injection was observed. While  $n_e$  is higher- and  $T_e$  is lower inside the separatrix for the  $\bar{n}_e/n_{eG} = 0.95$  timeslices than for similar measurements made in a non-puff case, we have found that the  $n_e T_e$  product is approximately the same for both non-puff and high density cases. In SNs, we have found that near the H–L transition  $T_e$  is often  $\leq 20$  eV with core MARFEs frequently present.

#### 4.4. Edge $n_e$ and $T_e$

The edge (or “pedestal”) electron temperature ( $T_{e,ped}$ ) has been suggested as an important ingredient in triggering the L–H transitions [13]. It has been further noted that the edge  $T_e$  at the H–L transition is approximately equal to the original edge  $T_e$  at the L–H transition [14]. Our data supports these contentions for the DN and SN cases examined. For example, the SN and DN

plasmas in Fig. 6 had nearly identical  $I_p$ ,  $P_{inj}$ , and  $B_T$ ;  $\Gamma_{D2}$  for the DN was slightly higher, i.e., 120 versus 105 Torr l/s. Prior to gas injection, both discharges had type I “giant” ELMs with frequency of 60–70 Hz and  $\tau_E \cong 170$  ms. The L–H and the H–L transitions are indicated for each configuration.  $T_{e,ped}$  for both cases underwent large excursions between their L–H and H–L transitions [Fig. 6(a)]. Yet, for both configurations,  $T_{e,ped}$  was approximately the same at their respective L–H and H–L transition points. We have also compared the electron temperature profile near the plasma edge and found them to be virtually identical for the SN and DN cases near their H–L backtransition.

Pedestal electron density ( $n_{e,ped}$ ), as expected, differed significantly at their respective L–H and H–L transition points [Fig. 6(b)]. Note that both  $n_{e,ped}$  and the normalized line-averaged density  $\bar{n}_e/n_{e,G}$  [Fig. 6(c)] for the DN at the H–L backtransition were approximately 15%–20% above those for the SN. Figure 6(c) also shows that the density in the DN increased at over twice the rate in the SN. In general, DNs tend to fuel at a faster rate, as we discuss in the next section.

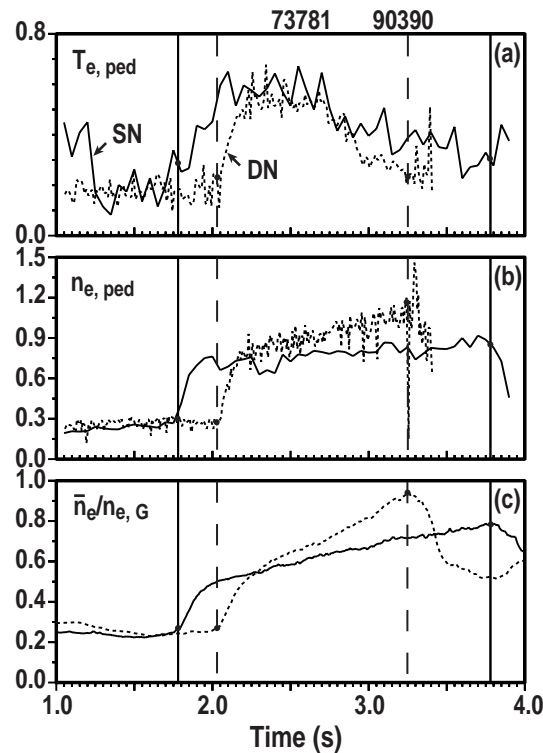


Fig. 6. (a)  $T_{e,ped}$  at the L–H and H–L transitions are similar for both SN (solid) and DN (dashed) divertors. (b)  $n_{e,ped}$  and (c)  $\bar{n}_e/n_{e,G}$  increase significantly faster in the DN case during gas injection:  $I_p = 1.5$  MA,  $B_T = 2.1$  T,  $\kappa = 2.0$ ,  $q_{95} \sim 4.5$ , and  $P_{inj} \sim 7.2$  MW. Gas injection for the SN started at  $t = 2.3$  s and for the DN at  $t = 2.7$  s.

## 5. DISCUSSION

Fueling by gas puffing in DN configurations is more efficient than in SNs. This may be due a combination of better direct (“first flight”) fueling and improved access of the neutrals to the core plasma for the DNs. To show this is plausible, we use a simple particle balance model:

$$dN_i/dt = S_{NBI} + \gamma S_{gas} - N_i/\tau_p \times (1 - R) \quad , \quad (1)$$

where  $N_i$  is the total ion particle content of the core plasma,  $S_{NBI}$  is the rate of beam particles ionizing inside the core plasma,  $S_{gas}$  is the gas puffing rate,  $\gamma$  is the fraction of gas puffed neutrals penetrating the core plasma directly from the gas injector,  $\tau_p$  is the particle confinement time of the core plasma, and  $R$  is the fraction of recycled neutrals coming back into the core plasma after recycling.

We estimate  $N_i/\tau_p$  for the cases described in Fig. 6 by first finding a self-consistent pair  $\chi_{eff}$  and  $\alpha$ , where  $\chi_{eff}$  is the anomalous perpendicular diffusivity for thermal energy,  $\alpha = 2.5 D_{\perp}/\chi_{eff}$ , and  $D_{\perp}$  is the anomalous perpendicular diffusivity for particles. We follow Porter’s approach [15], using the measured gradients in the density and temperature at the separatrix and the estimated power across the separatrix. We estimate  $\gamma$  computing the ionization mean free path for Franck-Condon neutrals (~3 eV), using the exponential scrapeoff  $n_e$  and  $T_e$  profiles from Thomson scattering and electron impact ionization data [16]. The results, shown in Table 1 suggest that roughly half of the improved fueling in DNs may be due to more efficient (direct) fueling and the other half may be due to the fact that a recycled neutral has a greater probability of re-entering the core (as opposed to being “pumped” by the graphite tiles).

**Table 1**  
**Particle balance: SN versus DN**

	SN	DB
$dN_i/dt$ (amps)	50	125
$S_{NBI}$ (amps)	160	160
$\gamma$	0.045	0.065
$S_{gas}$ (amps)	1100	1320
$N_i/\tau_p \times (1 - R)$ (amps)	160	121
$R$	0.800	0.865

While the above global analysis is useful in identifying possible sources for improved fueling in DNs, it does not explain *why* R is higher in the DN. To address this issue, we need to understand why the SN and DN discharges near their (high density) H–L backtransitions behave so differently. The absence of the PDD during routine high density DN operation is especially noteworthy. Key to understanding this behavior is the realization that neutral pressure in the private flux region at either end of the DN divertor is much lower than in a corresponding SN at high density. Neutral particle pressure in the PFR has been identified as an important ingredient in triggering the PDD regime by transferring plasma momentum away from the divertor separatrix, possibly by charge-exchange or ion-neutral collisions [17–19]. Ghendrih [18], for example, has argued that this is applicable to DIII–D SN gas puffed discharges where the neutrals reduce plasma pressure along the divertor separatrix by charge-exchanging with ions, and has established a scaling for the neutral pressure needed for triggering the PDD. The neutral pressure measured in the PFR of (either) divertor in DN high density discharges is less than that required neutral pressure predicted by Ghendrih as necessary for triggering the PDD. From this perspective, it is understandable that the DNs did not reach the PDD regime.

Neutral pressure in the PFR is much lower in DNs than comparable SNs. The SN divertor has measurable density in the PFR during gas puffing (particularly during the PDD). It is more difficult for recycled neutrals to penetrate through this density barrier out of the divertor and into the core. This density barrier then inhibits fueling in SNs. In the DNs we have examined, we see no evidence of comparable density in the private flux region. Moreover, fewer neutrals accumulate in the divertor, due to better fueling in the DNs.

It is unclear as to why significant density forms in the private flux region of SNs but does not in DNs. We speculate that, while both SNs and DNs “detach” along the inboard leg between ELMs (during gas puffing), ELMing events (briefly) re-attach the inboard leg. For SNs, continued gas puffing during the PDD resulted in an increase in ELM frequency and less time for the inboard leg to relax again to a detached state; hence, the ELMing pulse along the inboard leg helps build up neutral pressure in the PFR by both supplying recycling particles and then inhibiting their escape from the PFR through the inboard leg. On a qualitative level, ELMing events for DNs do not appear as “strong” in terms of particle (or heat) flux as SNs. Partly responsible for this may be that the particle and heat fluxes which flow to the high field side are divided between two poloidally separate locations in DNs, whereas these high field side flows are concentrated at a single poloidal location in SNs (i.e., “sharing” by the divertors). In addition, if the particle flux from the ELMs (or even between-ELM contributions) are ejected primarily into the weak toroidal field side of the plasma as suggested by the time difference of an ELM pulse arriving at the inner and outer strike points [20], then the ELM pulse can be “short-circuited” by either outboard divertor before it reaches the inboard divertors. We have measured

the power flow to the outboard divertors and found it significantly greater than that to the inboard divertors (e.g.,  $\sim 6\times$  before  $D_2$  injection). For SNs, this is  $\sim 2\times$  [21].

## **6. CONCLUSION**

We have shown that the road to the H-L backtransition for the single-null and double-null cases were very different, although their  $T_{e,ped}$  (or  $T_e$ -profile) were very similar at the back transition. We suspect that the detachment/reattachment of the inboard leg during ELMing conditions plays a pivotal role in the build-up of neutrals in the private flux region. Double-nulls are “more detached” along their inboard legs than corresponding single-nulls. Thus, neutrals in the private flux region for double-nulls have a higher probability of escaping to the inboard side of the plasma and have direct fueling access to the core plasma. Spreading out the ionization of neutrals along the inboard plasma in double-null appears to lead to more efficient fueling of the core than allowing neutrals to accumulate in the divertor, as in single-nulls. Future work in understanding the high density behavior of single-null and double-null discharges should focus on the cause(s) of the in/out asymmetries in the particle and heat flux at the divertor targets, both during and between ELMing events.

## REFERENCES

- [1] T.W. Petrie, *et al.*, Proc. 18th Europ. Conf. on Controlled Fusion and Plasma Physics, Berlin, Vol. 15C part III (1991) 237.
- [2] T.W. Petrie, *et al.*, J. Nucl. Mater. **196–198** (1992) 848.
- [3] T.W. Petrie, Nucl. Fusion **37** (1997) 321.
- [4] J. Drake, Phys. Fluids **30** (1987) 2429.
- [5] B. Lipschultz, *et al.*, J. Nucl. Mater. **220–222** (1995) 50.
- [6] G. Janeschitz, *et al.*, Proc. 19th Europ. Conf. on Controlled Fusion and Plasma Physics, Innsbruck, Vol. 16C part II (1993) 727.
- [7] M. Laux, Proc. 20th Europ. Conf. on Controlled Fusion and Plasma Physics, Lisbon, Vol. 17C part II (1993)
- [8] Fusion Engineering and Design **38** (1997)115–137, Special Issue: ARIES-RS Tokamak Power Plant Design (1997).
- [9] M. Greenwald, J. Terry, S. Wolfe, *et al.*, Nucl. Fusion **28** (1988) 2199.
- [10] P.N. Yushmanov, *et al.*, Nucl. Fusion **30** (1990) 1999.
- [11] T.W. Petrie, *et al.*, “Behavior of Double-Null H-mode Discharges at High Density in DIII-D,” 39th Annual Meeting of the Am. Phys. Soc., Div. of Plasma Phys. **42** (1997) 1919.
- [12] T.W. Petrie, *et al.*, J. Nucl. Mater. **241–243** (1997) 639.
- [13] ASDEX Team, Nucl. Fusion **29** (1989) 1959.
- [14] H. Zohm, *et al.*, Fusion Energy 1996 (Proc. 16th Int. Conf. Montreal, 1996) Vol 1, IAEA, Vienna (1996) 439.
- [15] G.D. Porter, “Role of Particle Flow on Power Balance on DIII-D,” (submitted to Phys. Plasmas).
- [16] R. Freeman, E. Jones, CLM-R-137, Culham Laboratory, Abingdon (1977).
- [17] P.C. Stangeby, Nucl. Fusion **33** (1993) 1695.
- [18] Ph. Ghendrih, *et al.*, J. Nucl. Mater. **220–222** (1995) 305.
- [19] Ph. Ghendrih, *et al.*, Proc. 15th International Conf. on Plasma Physics and Contr. Nucl. Fusion res., Seville, Vol 3 (1994) 441.
- [20] D.N. Hill, *et al.*, Nucl. Fusion **28** (1988) 902.
- [21] A.W. Leonard, *et al.*, J. Nucl. Mater. **220–222** (1995) 325.

## **ACKNOWLEDGMENT**

Work supported by U.S. Department of Energy under Contracts DE-AC03-89ER51114, W-7405-ENG-48, DE-AC05-96OR22464, and Grant No. DE-FG03-95ER54294.